Space-Time Geostatistical Models with both Linear and Seasonal Structures in the Temporal Components

Alfredo Alegría * and Emilio Porcu †
Department of Mathematics, University Federico Santa Maria, Valparaiso, Chile.

February 14, 2017

Abstract

We provide a novel approach to model space-time random fields where the temporal argument is decomposed into two parts. The former captures the linear argument, which is related, for instance, to the annual evolution of the field. The latter is instead a circular variable describing, for instance, monthly observations. The basic intuition behind this construction is to consider a random field defined over space (a compact set of the d-dimensional Euclidean space) across time, which is considered as the product space $\mathbb{R} \times \mathbb{S}^1$, with $\mathbb{S}^1$ being the unit circle. Under such framework, we derive new parametric families of covariance functions. In particular, we focus on two classes of parametric families. The former being parenthetical to the Gneiting class of covariance functions. The latter is instead obtained by proposing a new Lagrangian framework for the space-time domain considered in the manuscript. Our findings are illustrated through a real dataset of surface air temperatures. We show that the incorporation of both temporal variables can produce significant improvements in the predictive performances of the model. We also discuss the extension of this approach for fields defined spatially on a sphere, which allows to model space-time phenomena over large portions of planet Earth.

Keywords: Gneiting class; Lagrangian framework; Spherical harmonics; Temperatures.

*alfredo.alegria@usm.cl
†emilio.porcu@usm.cl

1 Introduction

Geostatistical approaches have become a popular methodology to model phenomena related to climatology, environmental sciences, oceanography, and many other branches of applied sciences. The observations are typically assumed as a partial realization of a stationary space-time Gaussian random field (GRF), namely $\{Z(\boldsymbol{x}, t) : \boldsymbol{x} \in \mathcal{D}, t \in \mathcal{T}\}$, where $\mathcal{D}$ denotes the spatial domain and $\mathcal{T}$ denotes the temporal horizon (see Stein, 2005, Gneiting et al., 2007 and Cressie and Wikle, 2015).

The review in Gneiting et al. (2007) provides a complete picture of stationary space-time GRFs, focusing on the case where $\mathcal{D} \subset \mathbb{R}^d$ and $\mathcal{T} \subset \mathbb{R}$. The authors claim that this is the natural domain for a space-time model. Indeed, in many situations this approach is appropriate. However, it might be of limited applicability, for instance, when dealing with monthly observations along several years, since in this case cyclic temporal patterns would not be taken into account. Past literature has been focused in incorporating the cyclic component in the trend of the field and then removing it through standard techniques (see, for instance, Haslett and Raftery, 1989 for the analysis of wind speed data). Another appealing option is to consider non-stationarity in the temporal component in order to capture non-negligible effects of the monthly scale. At the same time, non-stationary models have been less explored in the literature, with the work of Fuentes et al. (2008) being a notable exception.

A similar limitation arises when only cyclic patterns are considered. Shirota and Gelfand (2016) develop space-time point pattern models with temporal variable having a cyclical behavior, but again, this approach does not simultaneously capture the linear and circular structure described above.

We propose a strategy to model the duality in the temporal evolution of a spatial field. Our proposal directly incorporates the cyclic patterns in the domain of the field. Specifically, we consider a space-time model with two different temporal variables. The former is the classical real variable as being considered by most part of the space-time literature, which represents the linear evolution of the field. The latter is a circular variable related to cyclic behaviors. Such circular temporal variable is taken on the unit circle, with the corresponding geodesic (or great circle) metric. For instance, in monthly data, this notion of distance allows to distinguish that November and January are equally separated from December, whereas the linear temporal variable is not individually able to capture such structure.

The covariance functions associated to these kinds of fields must incorporate an additional argument reserved for the seasonal temporal component. According to this principle, we derive some non-separable families of covariances of the Gneiting type (Gneiting, 2002). The proposed models admit different scale parameters for each temporal variable, as well as for the spatial variable.

We additionally study transport effects (or Lagrangian) models according to the new framework proposed in the paper. These models provide a natural representation for phenomena with prevailing winds or ocean currents (Gupta and Waymire, 1987; Cox and Isham, 1988; Alegria and Porcu, 2016). We provide two alternative generalizations of the classical Lagrangian approach. In particular, we obtain additional covariances with closed form expressions.

A real dataset of surface air temperatures over the Australian territory is then analyzed. The data are provided by the National Center for Atmospheric Research (NCAR), Boulder, CO, USA. We show that our proposal can generate significant improvements in the predic-

tive performance with respect to a model that only considers linear or cyclic evolutions.

For phenomena defined over large portions of planet Earth, it is necessary to take into account the curvature of the globe. We discuss the extension of our proposal for space-time fields defined spatially on spheres (see Gneiting, 2013, Porcu et al., 2016 and Alegría et al., 2017). The main challenge of this extension is that the covariances must depend spatially on the geodesic distance, which is the most natural metric to be considered over the spherical surface.

The remainder of the article is organized as follows. In Section 2 we describe the proposed space-time model. Section 3 contains some general classes of Gneiting type covariances. In Section 4 we propose two generalizations of the Lagrangian model. Section 5 focuses on a real data example, where we illustrate the improvements in the predictive performance when we take into account the duality in the temporal evolution. The extension of this approach for fields defined spatially on spheres is discussed in Section 6.

2 Space-time models with both linear and seasonal temporal evolution

This section introduces the background material as well as the methodological architecture behind the main results described subsequently. Throughout, $\mathbb{S}^1 = \{\boldsymbol{y} \in \mathbb{R}^2 : \|\boldsymbol{y}\| = 1\}$ denotes the unit circle embedded in the plane and $\|\cdot\|$ is the corresponding Euclidean norm. Let d be a positive integer. We consider a space-time GRF on the product space $\mathbb{R}^d \times \mathbb{R} \times \mathbb{S}^1$ and defined through the uncountable collection

$$\{Z(\boldsymbol{x}, t_l, \boldsymbol{t}_c) : \boldsymbol{x} \in \mathbb{R}^d, t_l \in \mathbb{R}, \boldsymbol{t}_c \in \mathbb{S}^1\},$$

where $\boldsymbol{x}$ denotes the spatial variable, t_l is the linear temporal variable and $\boldsymbol{t}_c$ is a circular temporal variable. Here, the idea is that t_l allows to model the linear temporal evolution of the field, whereas $\boldsymbol{t}_c$ represents the seasonal behavior.

2.1 Stationary covariance functions

We use the notation $u_c := u_c(\boldsymbol{t}_c, \boldsymbol{t}'_c) = \arccos\langle \boldsymbol{t}_c, \boldsymbol{t}'_c \rangle \in [0, \pi]$ for the geodesic distance between any pair of circular instants $\boldsymbol{t}_c$ and $\boldsymbol{t}'_c$ on $\mathbb{S}^1$. Here, $\langle \cdot, \cdot \rangle$ is the standard inner product on $\mathbb{R}^2$. We call the covariance structure of Z *stationary* if there exists a mapping $C : \mathbb{R}^d \times \mathbb{R} \times [0, \pi] \to \mathbb{R}$ such that

$$C(\boldsymbol{h}, u_l, u_c) = \mathrm{cov}\{Z(\boldsymbol{x}, t_l, \boldsymbol{t}_c), Z(\boldsymbol{x}', t'_l, \boldsymbol{t}'_c)\}, \qquad \boldsymbol{x}, \boldsymbol{x}' \in \mathbb{R}^d, \quad t_l, t'_l \in \mathbb{R}, \quad \boldsymbol{t}_c, \boldsymbol{t}'_c \in \mathbb{S}^1, \tag{2.1}$$

where $\boldsymbol{h} = \boldsymbol{x} - \boldsymbol{x}'$, $u_l = t_l - t'_l$ and $u_c := u_c(\boldsymbol{t}_c, \boldsymbol{t}'_c)$. In particular, we follow Alegría et al. (2017) when calling C *geodesically isotropic* with respect to the circular temporal component.

Covariance functions are positive definite. Formally stated, for any positive integer n, for any n-dimensional system of points $\{(\boldsymbol{x}_1, t_{l,1}, \boldsymbol{t}_{c,1}), \ldots, (\boldsymbol{x}_n, t_{l,n}, \boldsymbol{t}_{c,n})\} \subset \mathbb{R}^d \times \mathbb{R} \times \mathbb{S}^1$, and for any n-dimensional collection of constants $a_1, \ldots, a_n \in \mathbb{R}$, the following inequality holds

$$\sum_{i=1}^{n} \sum_{j=1}^{n} a_i a_j C(\boldsymbol{x}_i - \boldsymbol{x}_j, t_{l,i} - t_{l,j}, u_c(\boldsymbol{t}_{c,i}, \boldsymbol{t}_{c,j})) \geq 0. \tag{2.2}$$

Through the paper we work with mean square continuous random fields, Z. Arguments in Berg and Porcu (2016) show that the continuous mappings C associated to Z admit a

uniquely determined series expansion of the type

$$C(\boldsymbol{h}, u_l, u_c) = \sum_{n=0}^{\infty} \varphi_n(\boldsymbol{h}, u_l)\mathcal{T}_n(\cos u_c), \qquad (\boldsymbol{h}, u_l, u_c) \in \mathbb{R}^d \times \mathbb{R} \times [0, \pi], \tag{2.3}$$

where $\mathcal{T}_n$ is the Tchebyshev polynomial of degree n (Abramowitz and Stegun, 1970) and $\{\varphi_n\}_{n=0}^{\infty}$ is a sequence of valid stationary covariance functions on $\mathbb{R}^d \times \mathbb{R}$, with $\sum_{n=0}^{\infty} \varphi_n(\mathbf{0}, 0) < \infty$. Additionally, classical Fourier inversion shows that

$$\begin{aligned} \varphi_0(\boldsymbol{h}, u_l) &= \frac{1}{\pi} \int_0^{\pi} C(\boldsymbol{h}, u_l, u_c) \mathrm{d}u_c, \\ \varphi_n(\boldsymbol{h}, u_l) &= \frac{2}{\pi} \int_0^{\pi} C(\boldsymbol{h}, u_l, u_c)\mathcal{T}_n(\cos u_c) \mathrm{d}u_c, \qquad n \geq 1. \end{aligned}$$

A relevant remark is that, in virtue of Bochner's Theorem (Bochner, 1955), Equation (2.3) can be restated in terms of classical Fourier transforms

$$C(\boldsymbol{h}, u_l, u_c) = \sum_{n=0}^{\infty} \int_{\mathbb{R}^d \times \mathbb{R}} \exp\{-\imath\langle \boldsymbol{h}, \boldsymbol{\omega}\rangle - \imath u_l \tau\}\mathcal{T}_n(\cos u_c) \mathrm{d}F_n(\boldsymbol{\omega}, \tau), \tag{2.4}$$

where $\{F_n\}_{n=0}^{\infty}$ is a sequence of finite, non-negative and symmetric measures on $\mathbb{R}^d \times \mathbb{R}$, and $\imath \in \mathbb{C}$ denotes the unit imaginary number. Some more remarks are in order. For any covariance function C on $\mathbb{R}^d \times \mathbb{R} \times \mathbb{S}^1$, the margins $C(\mathbf{0}, \cdot, \cdot)$, $C(\cdot, 0, \cdot)$, $C(\cdot, \cdot, 0)$ are covariance functions on lower dimensional spaces. Same thing holds for the margins $C(\mathbf{0}, 0, \cdot)$, $C(\mathbf{0}, \cdot, 0)$ and $C(\cdot, 0, 0)$. For all of these special cases, integral and series representations can be obtained by applying Equation (2.1). Apparently, if the function C in Equation (2.4) is radially symmetric in the first argument and symmetric in the second, then simplified expressions can be obtained in virtue of the arguments used in Daley and Porcu (2014) with the references therein.

2.2 Separability and full symmetry revisited

The easiest way to construct valid covariance models is through separable covariance structures. The more general framework proposed in this manuscript inspires for new definitions, that we illustrate as follows.

- We say that the covariance C defined through Equation (2.1) is *space versus time separable* if there exist two mappings $C_1 : \mathbb{R}^d \to \mathbb{R}$ and $C_2 : \mathbb{R} \times [0, \pi] \to \mathbb{R}$ such that

$$C(\boldsymbol{h}, u_l, u_c) = C_1(\boldsymbol{h})C_2(u_l, u_c), \qquad (\boldsymbol{h}, u_l, u_c) \in \mathbb{R}^d \times \mathbb{R} \times [0, \pi].$$

- The covariance C is called *linear versus circular time separable* if there exist two mappings $C_1 : \mathbb{R}^d \times \mathbb{R} \to \mathbb{R}$ and $C_2 : \mathbb{R}^d \times [0, \pi] \to \mathbb{R}$ such that

$$C(\boldsymbol{h}, u_l, u_c) = C_1(\boldsymbol{h}, u_l)C_2(\boldsymbol{h}, u_c), \qquad (\boldsymbol{h}, u_l, u_c) \in \mathbb{R}^d \times \mathbb{R} \times [0, \pi].$$

- Finally, we call C *fully separable* if there exist three mappings $C_1 : \mathbb{R}^d \to \mathbb{R}$, $C_2 : \mathbb{R} \to \mathbb{R}$ and $C_3 : [0, \pi] \to \mathbb{R}$ such that

$$C(\boldsymbol{h}, u_l, u_c) = C_1(\boldsymbol{h})C_2(u_l)C_3(u_c), \qquad (\boldsymbol{h}, u_l, u_c) \in \mathbb{R}^d \times \mathbb{R} \times [0, \pi].$$

Some comments are in order. The works developed by Gneiting (2002), Gneiting (2013) and Porcu et al. (2016) represent the building blocks for more sophisticated models. The advantage of separability assumptions is that they allow factorizations of the covariance matrices and thus for fast computations. At the same time, separability is often considered an unrealistic property. In general, we are interested in non-separable models since they allow to model more complex space-time dependencies.

Since we are working under the assumption of geodesic isotropy in the circular temporal variable, it does not make sense to talk about symmetry with respect to such component.

Thus, the concept of full symmetry discussed in Gneiting (2002) and Gneiting et al. (2007) is completely analogous in this context. In fact, the stationary covariance function C is called fully symmetric if

$$C(\boldsymbol{h}, u_l, u_c) = C(-\boldsymbol{h}, u_l, u_c) = C(\boldsymbol{h}, -u_l, u_c) = C(-\boldsymbol{h}, -u_l, u_c),$$

for all $(\boldsymbol{h}, u_l, u_c) \in \mathbb{R}^d \times \mathbb{R} \times [0, \pi]$. In particular, from Equation (2.4) we can see how the full symmetry condition depends on the sequence of functions $\{\varphi_n\}_{n=0}^{\infty}$. A direct implication of Theorem 4.3.2 in Gneiting et al. (2007) is that any stationary and fully symmetric covariance can be written as

$$C(\boldsymbol{h}, u_l, u_c) = \sum_{n=0}^{\infty} \int_{\mathbb{R}^d \times \mathbb{R}} \cos(\langle \boldsymbol{h}, \boldsymbol{\omega} \rangle) \cos(u_l \tau) \mathcal{T}_n(\cos u_c) \mathrm{d}F_n(\boldsymbol{\omega}, \tau), \tag{2.5}$$

where $\{F_n\}_{n=0}^{\infty}$ is a sequence of finite, non-negative and symmetric measures on $\mathbb{R}^d \times \mathbb{R}$.

3 Non-separable covariance functions of the Gneiting type

This section provides new parametric families of covariance functions for the proposed framework. A mapping $g : [0, \infty) \to (0, \infty)$ is called *completely monotone* if it is infinitely differentiable on $(0, \infty)$ and $(-1)^n g^{(n)}(r) \geq 0$, for all $n \in \mathbb{N}$ and $r \geq 0$. On the other hand, a mapping $f : [0, \infty) \to (0, \infty)$ is called a *Bernstein* function if it is a positive function with completely monotone derivative. For a more detailed study of the properties of these functions, we refer the reader to Porcu and Schilling (2011).

The following result generalizes the Gneiting class (Gneiting, 2002) and is provided by Alegría et al. (2017) under the framework of multivariate random fields. Here, we adapt

such a result to our framework. Throughout, $f|_{[0,\pi]}$ denotes the restriction of the mapping f to the interval $[0,\pi]$.

Theorem 3.1. (Alegría et al., 2017) Let d be a positive integer, g a completely monotone function and f_i, for $i=1,2$, Bernstein functions. Then,

$$C(\boldsymbol{h},u_l,u_c)=\frac{1}{\{f_2(u_c)|_{[0,\pi]}\}^{1/2}\left\{f_1\left[\frac{u_l^2}{f_2(u_c)|_{[0,\pi]}}\right]\right\}^{d/2}}g\left(\frac{\|\boldsymbol{h}\|^2}{f_1\left[\frac{u_l^2}{f_2(u_c)|_{[0,\pi]}}\right]}\right), \tag{3.1}$$

for $(\boldsymbol{h},u_l,u_c)\in\mathbb{R}^d\times\mathbb{R}\times[0,\pi]$, is a covariance function.

For the proof of Theorem 3.1, we refer the reader to Alegría et al. (2017). Here, $C(\boldsymbol{h},u_l,0)$ reduces to the celebrated Gneiting class (Gneiting, 2002). Tables 3.1 and 3.2 contain a list of completely monotone and Bernstein functions, respectively.

Our original contribution is now focused on a different Gneiting type covariance. Following Porcu et al. (2016), we call this covariance a modified Gneiting class.

Theorem 3.2. Let n and d be positive integers. Let $g:[0,\infty)\to(0,\infty)$ be a completely monotone function. Consider $f_i:[0,\infty)\to(0,\infty)$, $i=1,2$, strictly increasing and concave functions. Then, the mapping defined through

$$C(\boldsymbol{h},u_l,u_c)=\frac{1}{\{f_1(\|\boldsymbol{h}\|)f_2(|u_l|)\}^{n+2}}g\left(u_cf_1(\|\boldsymbol{h}\|)f_2(|u_l|)\right), \tag{3.2}$$

for $(\boldsymbol{h},u_l,u_c)\in\mathbb{R}^d\times\mathbb{R}\times[0,\pi]$, is a covariance function.

The proof of Theorem 3.2 is deferred to Appendix A.

Example 3.1. Consider the model (3.1). The first entries in Tables 3.1 and 3.2 allow to generate the covariance

$$C(\boldsymbol{h},u_l,u_c)=\frac{\sigma^2}{\left(\frac{400u_c}{b_c}+1\right)^{1/2}\left(\frac{20|u_l|/b_l}{\left(\frac{400u_c}{b_c}+1\right)^{1/2}}+1\right)}\exp\left\{-\frac{3\|\boldsymbol{h}\|/\phi}{\left(\frac{20|u_l|/b_l}{\left(\frac{400u_c}{b_c}+1\right)^{1/2}}+1\right)^{1/2}}\right\}, \tag{3.3}$$

Table 3.1: A list of completely monotone functions with the corresponding parameter restrictions. Here, K_ν denotes the modified Bessel function of second kind of degree ν.

Function	Parameters restriction
$g(t) = \exp(-ct^\gamma)$	$c > 0$, $0 < \gamma \leq 1$
$g(t) = (2^{\nu-1}\Gamma(\nu))^{-1}(c\sqrt{t})^\nu K_\nu(c\sqrt{t})$	$c > 0$, $\nu > 0$
$g(t) = (1 + ct^\gamma)^{-\nu}$	$c > 0$, $0 < \gamma \leq 1$, $\nu > 0$
$g(t) = 2^\nu(\exp(c\sqrt{t}) + \exp(-c\sqrt{t}))^{-\nu}$	$c > 0$, $\nu > 0$

Table 3.2: A list of Bernstein functions with the corresponding parameter restrictions.

Function	Parameters restriction
$f(t) = (at^\alpha + 1)^\beta$	$a > 0$, $0 < \alpha \leq 1$, $0 \leq \beta \leq 1$
$f(t) = \ln(at^\alpha + b)/\ln(b)$	$a > 0$, $b > 1$ $0 < \alpha \leq 1$
$f(t) = (at^\alpha + b)/(b(at^\alpha + 1))$	$a > 0$, $0 < b \leq 1$, $0 < \alpha \leq 1$

where $(\boldsymbol{h}, u_l, u_c) \in \mathbb{R}^d \times \mathbb{R} \times [0, \pi]$. Here, ϕ, b_l and b_c are positive scale parameters, whereas $\sigma^2 > 0$ controls the variance of the field.

Example 3.2. Consider the model (3.2). Again, the first entries in Tables 3.1 and 3.2 allow to generate the covariance

$$C(\boldsymbol{h}, u_l, u_c) = \frac{\sigma^2}{\left[\left(1 + \frac{1.7\|\boldsymbol{h}\|}{\phi}\right)\left(1 + \frac{1.7\|u_l\|}{b_l}\right)\right]^3} \exp\left\{-\frac{3u_c}{b_c}\left(1 + \frac{1.7\|\boldsymbol{h}\|}{\phi}\right)\left(1 + \frac{1.7\|u_l\|}{b_l}\right)\right\}, \tag{3.4}$$

with $(\boldsymbol{h}, u_l, u_c) \in \mathbb{R}^d \times \mathbb{R} \times [0, \pi]$. Here, parameters ϕ, b_l, b_c and σ^2 have the same interpretation as in the previous example.

The parameterizations used in the previous examples imply that $C(\boldsymbol{h}, 0, 0)$, $C(\boldsymbol{0}, u_l, 0)$ and $C(\boldsymbol{0}, 0, u_c)$ are less than 0.05 for $\|\boldsymbol{h}\| > \phi$, $|u_l| > b_l$ and $u_c > b_c$, respectively. In Figure 3.1, we illustrate the contour lines for covariances (3.3) and (3.4), with $\sigma^2 = 1$, $\phi = 2$, $b_l = 20$ and $b_c = 10$. Figure 3.2 depicts four different realizations from model (3.4), with 1600 spatial locations on the squared $[0, 1]^2$, two linear and two circular time instants. We consider $\phi = 0.5$ and the following cases:

(a) Strong correlation in both temporal variables: $(b_l, b_c) = (30, 30)$;

(b) Weak correlation in both temporal variables: $(b_l, b_c) = (0.01, 0.01)$;

(c) Weak correlation in the linear temporal variable and strong correlation in the circular temporal variable: $(b_l, b_c) = (0.01, 30)$;

(d) Strong correlation in the linear temporal variable and weak correlation in the circular variable: $(b_l, b_c) = (30, 0.01)$.

The characteristics of each case are clearly reflected in Figure 3.2.

Figure 3.1: Contour lines for the Gneiting covariance (3.3) (I) and the modified Gneiting class (3.4) (II).

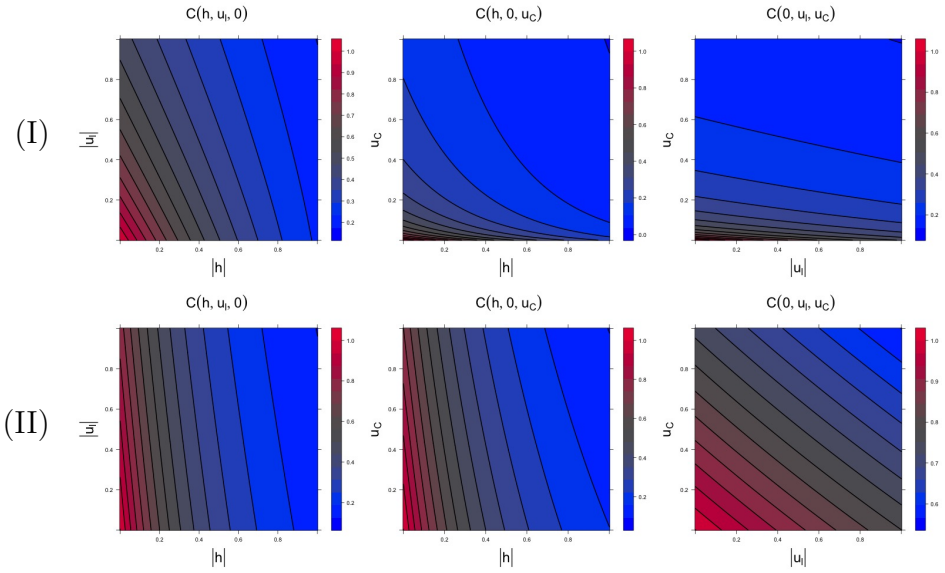

Figure 3.2: Simulated data from model (3.4), under scenarios (a)-(d), with 1600 spatial locations on the squared $[0, 1]^2$, two linear and two circular time instants.

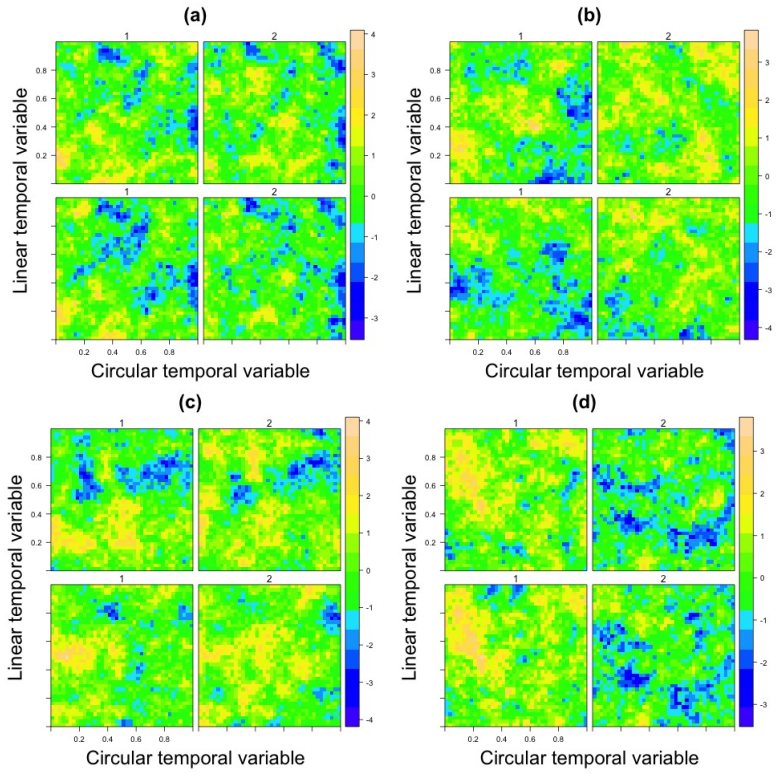

4 Generalized Lagrangian framework

We now focus on some generalizations of the Lagrangian model (Gupta and Waymire, 1987; Cox and Isham, 1988) in order to cover the framework proposed in this paper. We also derive some covariance functions with closed form expressions.

First generalization. We start with a space-time phenomena with a cyclic behavior in the temporal variable, namely $\{Y(\boldsymbol{x}, \boldsymbol{t}_c) : \boldsymbol{x} \in \mathbb{R}^d, \boldsymbol{t}_c \in \mathbb{S}^1\}$. Suppose that the covariance associated to Y is given by $C_Y(\boldsymbol{h}, u_c) := \text{cov}\{Y(\boldsymbol{x}, \boldsymbol{t}_c), Y(\boldsymbol{x}', \boldsymbol{t}_c')\}$, for $\boldsymbol{h} = \boldsymbol{x} - \boldsymbol{x}' \in \mathbb{R}^d$ and $u_c = u_c(\boldsymbol{t}_c, \boldsymbol{t}_c') \in [0, \pi]$. Let $t_l \in \mathbb{R}$ be a linear temporal variable and suppose that the entire field suffers a spatial displacement time-forward (in terms of t_l) with velocity determined by the random vector $\boldsymbol{V} \in \mathbb{R}^d$. Then, we have a generalized transport effect model given by

$$Z(\boldsymbol{x}, t_l, \boldsymbol{t}_c) = Y(\boldsymbol{x} - t_l \boldsymbol{V}, \boldsymbol{t}_c), \tag{4.1}$$

for $(\boldsymbol{x}, t_l, \boldsymbol{t}_c) \in \mathbb{R}^d \times \mathbb{R} \times \mathbb{S}^1$. The covariance function of Z is given by

$$C(\boldsymbol{h}, u_l, u_c) = \mathbb{E}_V\{C_Y(\boldsymbol{h} - u_l \boldsymbol{V}, u_c)\}, \qquad (\boldsymbol{h}, u_l, u_c) \in \mathbb{R}^d \times \mathbb{R} \times [0, \pi]. \tag{4.2}$$

When $\boldsymbol{V}$ is a Gaussian distributed random vector, we can generate closed form expressions. The following example is a straightforward generalization of a result reported by Schlather (2011).

Example 4.1. Let d be a positive integer, $\boldsymbol{\mu} \in \mathbb{R}^d$, Λ a symmetric positive definite matrix of order $d \times d$ and I_d the identity matrix. Let g be a completely monotone function and f a Bernstein function. Then,

$$C(\boldsymbol{h}, u_l, u_c) = \frac{1}{\left|u_l^2 \Lambda + f(u_c)|_{[0,\pi]} I_d\right|^{1/2}} g\left((\boldsymbol{h} - u_l \boldsymbol{\mu})^\top \left(u_l^2 \Lambda + f(u_c)|_{[0,\pi]} I_d\right)^{-1} (\boldsymbol{h} - u_l \boldsymbol{\mu}) \right), \tag{4.3}$$

Figure 4.1: Two simulated data from the transport effect model (4.3).

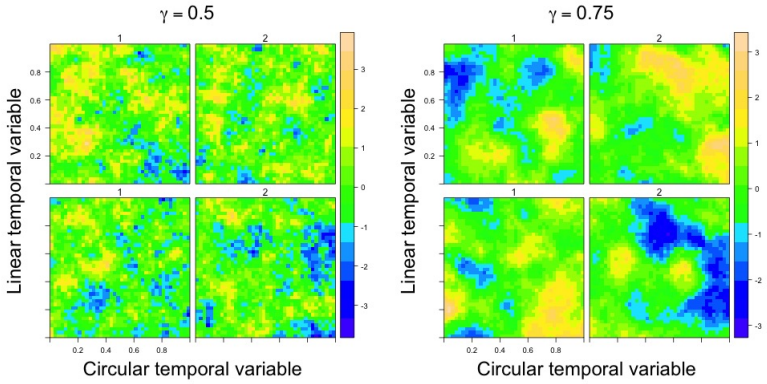

for $(\boldsymbol{h}, u_l, u_c) \in \mathbb{R}^d \times \mathbb{R} \times [0, \pi]$, is a valid covariance function.

We refer the reader to Appendix B for a detailed justification. Figure 4.1 depicts two simulations from the model given in Equation (4.3), with spatial locations on the squared $[0,1]^2$ and two linear and circular temporal instants, with $g(r) = \exp\{-r^\gamma\}$ and $f(r) = (1 + r^\alpha)$. For both cases, we consider $\boldsymbol{\mu} = (1,1)^\top$, $\Lambda = \begin{pmatrix} 1 & 1/2 \\ 1/2 & 2 \end{pmatrix}$ and $\alpha = 1$. The first simulation considers $\gamma = 1/2$, whereas the second $\gamma = 3/4$. The choice of γ determines the degree of smoothness of the sample paths.

Second generalization. Consider again the field Y as being previously defined, with covariance function given by the mapping $\tilde{C}_Y : \mathbb{R}^d \times [-1,1] \to \mathbb{R}$ defined through $\tilde{C}_Y(\boldsymbol{h}, \cos u_c) := \text{cov}\{Y(\boldsymbol{x}, \boldsymbol{t}_c), Y(\boldsymbol{x}', \boldsymbol{t}_c')\}$, for $\boldsymbol{h} = \boldsymbol{x} - \boldsymbol{x}' \in \mathbb{R}^d$ and $u_c = u_c(\boldsymbol{t}_c, \boldsymbol{t}_c') \in [0, \pi]$. Note that there is a subtle difference in the definition of the covariance function. Now, we develop an alternative formulation of a transport effect model. Suppose that the field suffers a shift effect in the variable $\boldsymbol{t}_c$ as t_l progresses. Such movement can be represented through a random rotation matrix $\mathcal{R}$ of order 2×2 and it must be proportional to t_l. Then, we have the

following generalization of the Lagrangian model

$$Z(\boldsymbol{x}, t_l, \boldsymbol{t}_c) = Y(\boldsymbol{x}, \mathcal{R}^{t_l}\boldsymbol{t}_c), \tag{4.4}$$

for $(\boldsymbol{x}, t_l, \boldsymbol{t}_c) \in \mathbb{R}^d \times \mathbb{R} \times \mathbb{S}^1$. Alegria and Porcu (2016) have studied these kind of constructions for Lagrangian models on spheres across time. The associated covariance is given by

$$\text{cov}\{Z(\boldsymbol{x}, t_l, \boldsymbol{t}_c), Z(\boldsymbol{x}', t_l', \boldsymbol{t}_c')\} = \mathbb{E}_{\mathcal{R}}\{C_Y(\boldsymbol{h}, \langle \boldsymbol{t}_c, \mathcal{R}^{u_l}\boldsymbol{t}_c' \rangle)\}, \tag{4.5}$$

where $\boldsymbol{h} = \boldsymbol{x} - \boldsymbol{x}'$ and $u_l = t_l - t_l'$.

Example 4.2. Note that the rotation matrix has the general form

$$\mathcal{R} = \begin{pmatrix} \cos\alpha & \sin\alpha \\ -\sin\alpha & \cos\alpha \end{pmatrix}$$

and we have two possible random movements (clockwise and anti-clockwise). Suppose that both opposite directions have associated the same probability. Thus, the covariance (4.5) is reduced to (see Alegria and Porcu, 2016)

$$C(\boldsymbol{h}, u_l, u_c) = \frac{1}{2}\left\{\tilde{C}_Y(\boldsymbol{h}, \cos(u_c + u_l\alpha)) + \tilde{C}_Y(\boldsymbol{h}, \cos(u_c - u_l\alpha))\right\}, \qquad (\boldsymbol{h}, u_l, u_c) \in \mathbb{R}^d \times \mathbb{R} \times [0, \pi]. \tag{4.6}$$

Some examples of the mapping $\tilde{C}_Y$ can be generated from the direct constructions developed in Porcu et al. (2016). For instance, a valid mapping $\tilde{C}_Y$ is a multiquadric type model

$$\tilde{C}_Y(\boldsymbol{h}, \xi) = \frac{1}{(1 + g^2(\|\boldsymbol{h}\|^2) - 2\xi g(\|\boldsymbol{h}\|^2))^{1/2}}, \qquad (\boldsymbol{h}, \xi) \in \mathbb{R}^d \times [-1, 1],$$

where $g : [0, \infty) \to (0, 1)$ is a completely monotone function.

5 Modeling surface air temperatures around Australia

We illustrate the use of the proposed framework on a space-time data set of surface air temperatures. The data come from the Community Climate System Model (CCSM4.0) (see Gent et al., 2011) provided by the National Center for Atmospheric Research (NCAR), Boulder, CO, USA.

The units for temperatures are Kelvin degrees. We consider 50 sites in the interval of longitudes $[70, 170]$ and latitudes $[-60, -10]$ degrees (see Figure 5.1). Note that such a region covers the Australian territory. We focus on 10 years in the range from December of 2002 to November of 2012. We consider four cyclic temporal instants: (Season 1) average of Dec-Feb, (Season 2) average of Mar-May, (Season 3) average of Jun-Aug and (Season 4) average of Sep-Nov. We model the average of each season as mutually equidistant points on a unit circle. In total, we have four cyclic instants per each year (40 temporal instants).

We remove through splines the spatial cyclic patterns along longitudes and latitudes in order to obtain a spatially stationary data set. The residuals are approximately Gaussian distributed with zero mean. Figure 5.1 shows the data set in the first three years. Note that for each fixed season there is a strong temporal linear correlation, whereas the cyclic temporal dependence is significant. In order to work with the proposed framework, we project the geographical coordinates onto the plane through the sinusoidal projection.

We consider three models

- A fully separable structure by taking the covariance

$$C(\boldsymbol{h}, u_l, u_c) = \frac{\sigma^2}{\left(\frac{400u_c}{b_c} + 1\right)^{1/2} \left(\frac{20|u_l|}{b_l} + 1\right)} \exp\left\{ -\frac{3\|\boldsymbol{h}\|/\phi}{\left(\frac{20|u_l|}{b_l} + 1\right)^{\beta/2}} \right\}, \tag{5.1}$$

Figure 5.1: Residuals of the surface air temperatures for each season for the first three years. Rows represent years and columns represent seasons. The 50 spatial locations considered in our study are indicated with black dots.

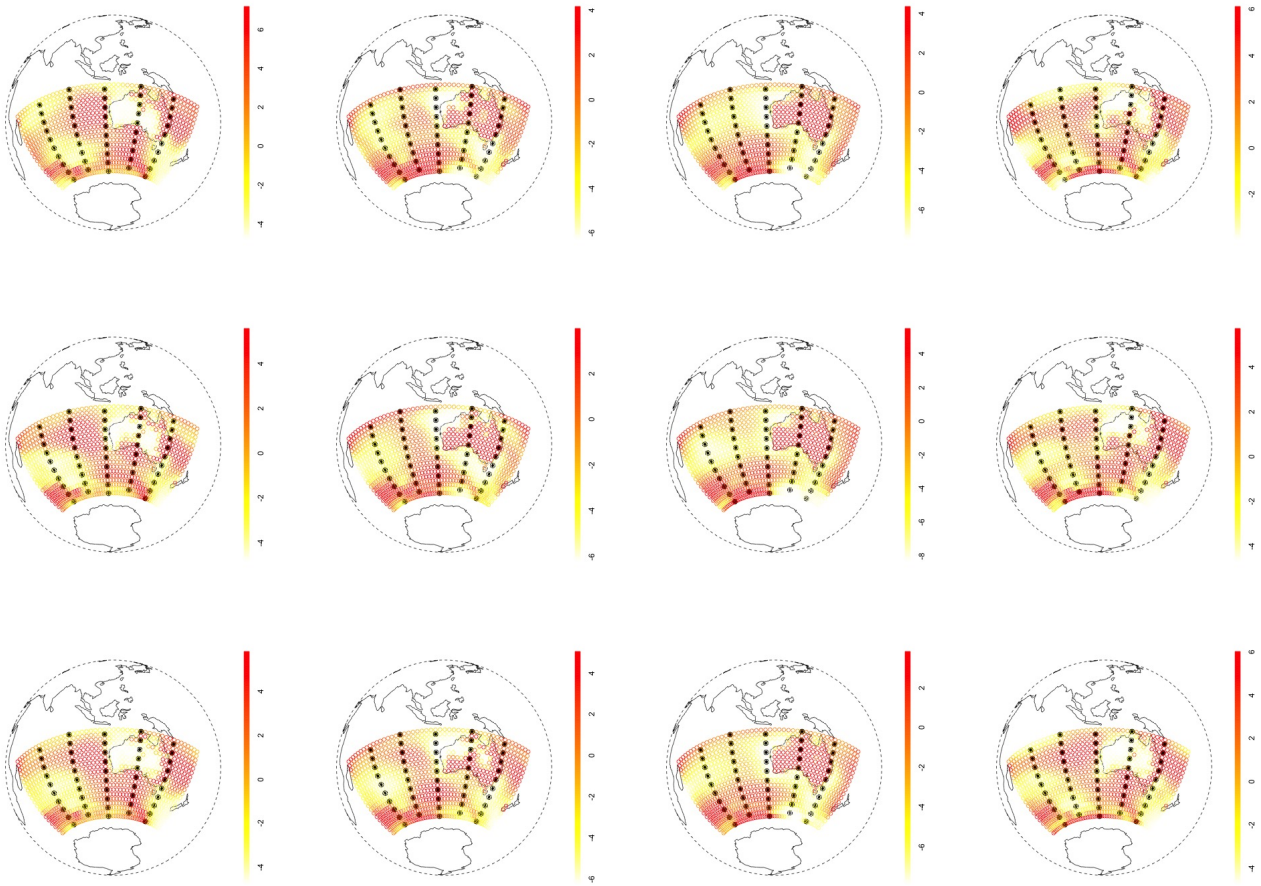

Table 5.1: Maximum likelihood estimates for each model. Standard errors are given in parentheses. We also report the Log-likelihood value at the optimum.

Model	$\widehat{\sigma}^2$	$\widehat{\phi}$	$\widehat{b_l}$	$\widehat{b_c}$	Log-likelihood
Fully separable	1.237	2872.098	91.123	82.651	252.854
	(0.083)	(179.886)	(7.312)	(15.760)	
Linear versus circular time separable	1.515	3626.895	132.062	80.961	255.077
	(0.108)	(195.858)	(10.677)	(15.543)	
Non-separable	1.726	3670.900	162.151	221.304	273.504
	(0.130)	(192.390)	(12.221)	(30.209)	

for $(\boldsymbol{h}, u_l, u_c) \in \mathbb{R}^2 \times \mathbb{R} \times \mathbb{S}^1$, with $\beta = 0$.

- A linear versus circular time separable structure by taking the covariance (5.1) with $\beta = 1$.
- A non-separable model given by Equation (3.3).

The vector of parameters is given by $(\sigma^2, \phi, b_l, b_c)^\top$. In Table 5.1, we report the maximum likelihood estimates for each model, with its associated standard error. We additionally show the Log-likelihood value attained at the optimum. The non-separable model presents better likelihood results than the separable ones. Figure 5.2 shows the empirical covariances versus the theoretical models at different linear and circular temporal lags.

We compare the predictive performance in terms of kriging through three different scenarios:

(A) Prediction using both linear and circular temporal evolution. Here, we use the three models described above.

Figure 5.2: Empirical covariances versus theoretical models at different linear and circular temporal lags.

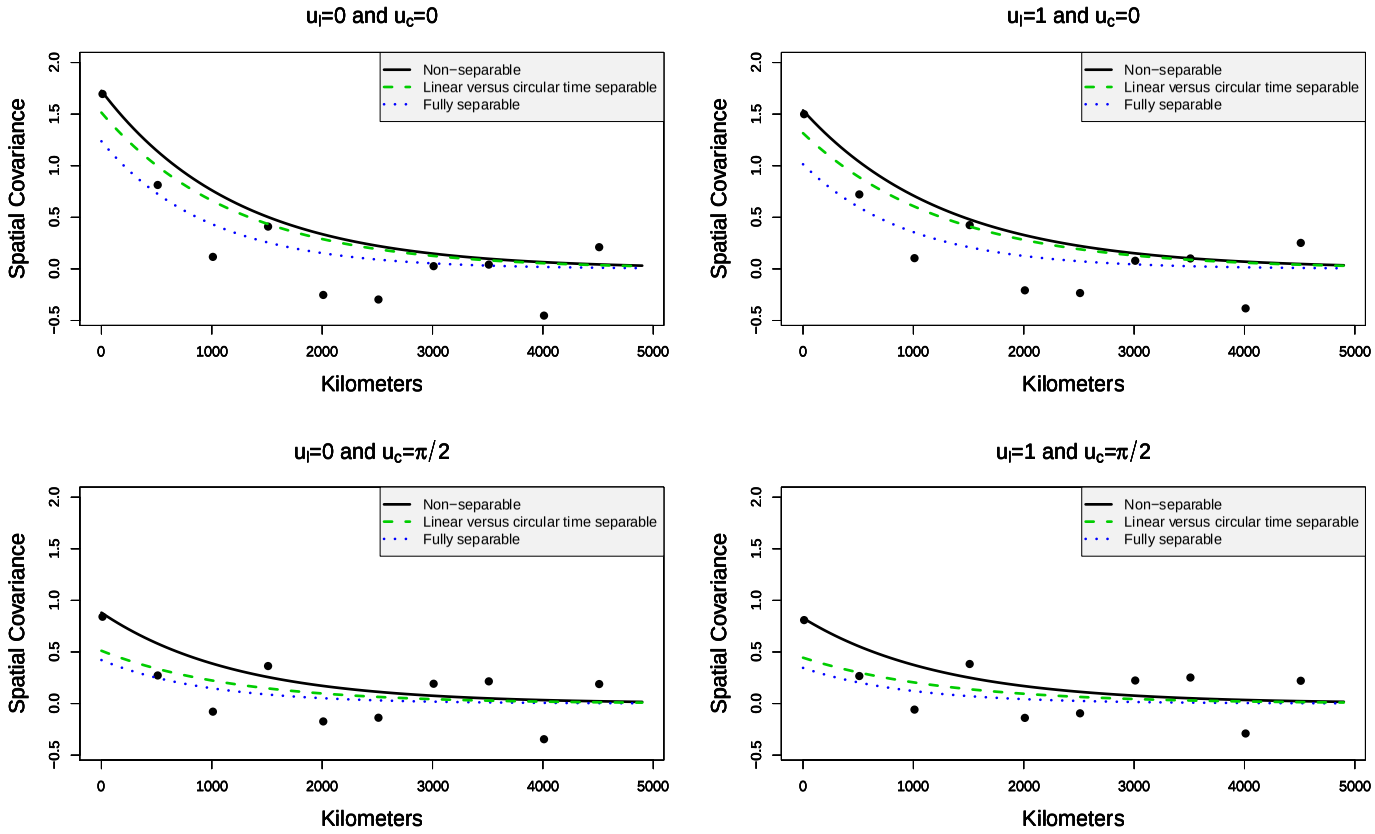

(B) Prediction for each fixed season using linear temporal evolution only. We consider the Gneiting class

$$C(\boldsymbol{h}, u_l) = \frac{\sigma^2}{\left(\frac{20|u_l|}{b_l} + 1\right)} \exp\left\{ -\frac{3\|\boldsymbol{h}\|/\phi}{\left(\frac{20|u_l|}{b_l} + 1\right)^{\beta/2}} \right\}, \qquad (\boldsymbol{h}, u_l) \in \mathbb{R}^d \times \mathbb{R},$$

with $\beta = 0$ (space versus time separable) and $\beta = 1$ (non-separable).

(C) Prediction for each fixed year using circular temporal evolution only. We consider a Gneiting type covariance

$$C(\boldsymbol{h}, u_c) = \frac{\sigma^2}{\left(\frac{400u_c}{b_c} + 1\right)^{1/2}} \exp\left\{ -\frac{3\|\boldsymbol{h}\|/\phi}{\left(\frac{400u_c}{b_c} + 1\right)^{\beta/2}} \right\}, \qquad (\boldsymbol{h}, u_c) \in \mathbb{R}^d \times [0, \pi],$$

with $\beta = 0$ (space versus time separable) and $\beta = 1$ (non-separable).

For all the exposed cases, interpretation of parameters is analogous.

We consider a drop-one prediction strategy and quantify the error in terms of the Mean Squared Error (MSE), the Log-Score (LSCORE) and the Continuous Ranked Probability Score (CRPS) (see Zhang and Wang, 2010). Smaller values of these indicators suggest better predictions. For Scenario B, we consider the average of the indicator across the four seasons, whereas for Scenario C we consider the average across the ten years. Thus, this strategy allows to compare the global prediction performance under each scenario.

Note that Scenario A generates significant predictive improvements with respect to Scenarios B and C. The strong correlation in the linear temporal variable implies that Scenario B is a reasonable choice but Scenario A generates a non-negligible reduction of 9.1% in terms of MSE with respect to Scenario B for the non-separable models. The performance of scenario C is quite poor in comparison to Scenarios A and B. Also, note that the non-separable models always outperform the separable ones.

Table 5.2: Predictive scores for Scenarios A-C.

Scenario	Model	MSE	LSCORE	CRPS
A	Fully separable	0.142	0.426	0.733
	Linear versus circular time separable	0.143	0.430	0.735
	Non-separable	0.140	0.420	0.732
B	Space versus time separable	0.155	0.450	0.771
	Non-separable	0.154	0.450	0.770
C	Space versus time separable	0.345	0.885	1.293
	Non-separable	0.319	0.847	1.248

6 Extension to global data

We finish the paper by studying the extension of our proposal to global data, where typically the space is the sphere $\mathbb{S}^2$ representing planet Earth. For the sake of completeness, we work with space-time GRFs defined spatially over a general d-dimensional unit sphere $\mathbb{S}^d := \{\boldsymbol{y} \in \mathbb{R}^{d+1} : \|\boldsymbol{y}\| = 1\}$. Consider a field Z defined as

$$\{Z(\boldsymbol{x}, t_l, \boldsymbol{t}_c) : \boldsymbol{x} \in \mathbb{S}^d, t_l \in \mathbb{R}, \boldsymbol{t}_c \in \mathbb{S}^1\}.$$

Under this context, the notion of stationarity requires a modification, and we say that the covariance function of Z is stationary if there exists a mapping $C : [0, \pi] \times \mathbb{R} \times [0, \pi] \to \mathbb{R}$ such that

$$C(\theta, u_l, u_c) = \text{cov}\{Z(\boldsymbol{x}, t_l, \boldsymbol{t}_c), Z(\boldsymbol{x}', t_l', \boldsymbol{t}_c')\},$$

where $\theta := \theta(\boldsymbol{x}, \boldsymbol{x}') = \arccos\langle \boldsymbol{x}, \boldsymbol{x}' \rangle \in [0, \pi]$ is the geodesic distance on $\mathbb{S}^d$, and where $(u_l, u_c) \in \mathbb{R} \times [0, \pi]$ have been defined in the previous sections. The following theorem characterizes completely the class of such continuous mappings C.

Before we state the result, we introduce some notation. The total mass of the uniquely determined rotation invariant surface measure ω_d on $\mathbb{S}^d$ is denoted as $\|\omega_d\| = \frac{2\pi^{(d+1)/2}}{\Gamma((d+1)/2)}$. Also, we define the constant $N_k(d) = \frac{(d)_{k-1}}{k!}(2k+d-1)$, for $k \geq 1$, and $N_0(d) = 1$. Here, Γ denotes the Gamma function and $(a)_k = a(a+1)\cdots(a+k-1)$, for $k \geq 1$ and $(a)_0 = 1$.

Theorem 6.1. Let d be a positive integer. The continuous mapping C is the stationary covariance associated to a field on $\mathbb{S}^d \times \mathbb{R} \times \mathbb{S}^1$ if and only if it admits the representation

$$C(\theta, u_l, u_c) = \sum_{n=0}^{\infty}\sum_{k=0}^{\infty} \varphi_{n,k}(u_l)\mathcal{T}_n(\cos u_c)\mathcal{G}_k^{(d-1)/2}(\cos\theta), \tag{6.1}$$

where $\mathcal{G}_n^{\lambda}$ is the λ-Gegenbauer polynomial of degree n, $\mathcal{T}_n$ is the Tchebyshev polynomial of degree n and $\{\varphi_{n,k}\}_{n,k=0}^{\infty}$ is a bi-sequence of valid stationary covariance functions on the real line such that $\sum_{n=0}^{\infty}\sum_{k=0}^{\infty}\varphi_{n,k}(0) < \infty$, given by

$$\varphi_{0,k}(u_l) = \frac{c_{k,d}}{\pi}\int_0^{\pi}\int_0^{\pi} C(\theta, u_l, u_c)\mathcal{G}_k^{(d-1)/2}(\cos\theta)(\sin\theta)^{d-1}\mathrm{d}u_c\mathrm{d}\theta,$$

for $k \geq 0$, and

$$\varphi_{n,k}(u_l) = \frac{2c_{k,d}}{\pi}\int_0^{\pi}\int_0^{\pi} C(\theta, u_l, u_c)\mathcal{T}_n(\cos u_c)\mathcal{G}_k^{(d-1)/2}(\cos\theta)(\sin\theta)^{d-1}\mathrm{d}u_c\mathrm{d}\theta,$$

for $n \geq 1$ and $k \geq 0$, where $c_{k,d} := \frac{N_k(d)\|\omega_{d-1}\|}{\|\omega_d\|}$.

Invoking Bochner's Theorem (Bochner, 1955), we can derive the following alternative expression for Equation (6.1)

$$C(\theta, u_l, u_c) = \sum_{n=0}^{\infty}\sum_{k=0}^{\infty}\int_{\mathbb{R}} \exp\{-\imath u_l\tau\}\mathcal{T}_n(\cos u_c)\mathcal{G}_k^{(d-1)/2}(\cos\theta)\mathrm{d}F_{n,k}(\tau), \tag{6.2}$$

where $\{F_{n,k}\}_{n=0}^{\infty}$ is a bi-sequence of finite, non-negative and symmetric measures on the real line.

Theorem 6.1 is a mixture between the results provided by Guella et al. (2015), on positive definite functions on product of spheres, and Berg and Porcu (2016) . The proof of Theorem 6.1 is deferred to Appendix C.

Acknowledgments

Alfredo Alegría is supported by Beca CONICYT-PCHA/Doctorado Nacional/2016-21160371. Emilio Porcu is supported by Proyecto Fondecyt Regular number 1130647.

We additionally acknowledge the World Climate Research Programme's Working Group on Coupled Modelling, which is responsible for Coupled Model Intercomparison Project (CMIP).

Appendices

A. Proof of Theorem 3.2

Consider the mappings

$$C_1(\boldsymbol{h}, u_c; \xi) = \frac{1}{[f_1(\|\boldsymbol{h}\|)]^{n+2}} \left(1 - \frac{u_c f_1(\|\boldsymbol{h}\|)}{\xi}\right)_+^{n+1}, \qquad \boldsymbol{h} \in \mathbb{R}^d, u_c \in [0, \pi], \xi \in \mathbb{R},$$

and

$$C_2(u_l; \xi) = \xi^{n+1}(1 - \xi f_2(|u_l|))_+^{\ell}, \qquad u_l \in \mathbb{R}, \xi \in \mathbb{R},$$

where $n \geq 1$ and $\ell \geq 1$ are integers and $(a)_+ = \max\{0, a\}$. Arguments in Porcu et al. (2016) and Alegría et al. (2017) show that $C_1(\cdot, \cdot; \xi)$ is a valid stationary covariance function on $\mathbb{R}^d \times \mathbb{S}^1$ for any $\xi \in \mathbb{R}$. Furthermore, $C_1(\boldsymbol{h}, u_c; \cdot)$ is an integrable mapping for any $(\boldsymbol{h}, u_c) \in \mathbb{R}^d \times [0, \pi]$. On the other hand, a criterion of the Pólya type (Daley et al., 2015 with the references therein) shows that $C_2(\cdot; \xi)$ is a valid covariance function on the real line, whereas $C_2(u_l; \cdot)$ is integrable on $\mathbb{R}$.

The scale mixture between C_1 and C_2 defined through

$$C_{\ell,n}(\boldsymbol{h}, u_l, u_c) := \int_{\mathbb{R}} C_1(\boldsymbol{h}, u_c; \xi) C_2(u_l; \xi) \mathrm{d}\xi$$

is a valid stationary covariance on $\mathbb{R}^d \times \mathbb{R} \times \mathbb{S}^1$. Following the arguments in Daley et al. (2015) we have that

$$C_{\ell,n}(\boldsymbol{h}, u_l, u_c) = \frac{\mathcal{B}(n+2, \ell+1)}{\{f_1(\|\boldsymbol{h}\|) f_2(|u_l|)\}^{n+2}} \left(1 - u_c f_1(\|\boldsymbol{h}\|) f_2(|u_l|)\right)_+^{n+\ell+1},$$

where $\mathcal{B}$ represents the Beta function. Since the class of positive definite functions is closed under pointwise convergence, the following mapping is a valid stationary covariance

$$\lim_{\ell \to \infty} C_{\ell,n}(\boldsymbol{h}, u_l, u_c/\ell) = \frac{\mathcal{B}(n+2, \ell+1)}{\{f_1(\|\boldsymbol{h}\|) f_2(|u_l|)\}^{n+2}} \exp\left(-u_c f_1(\|\boldsymbol{h}\|) f_2(|u_l|)\right).$$

Let us now recall that, by Bernstein's (1963) theorem (see Feller, 1966), any mapping $g : [0, \infty) \to (0, \infty)$ is completely monotone if and only if

$$g(t) = \int_{[0,\infty)} \exp\{-rt\} \mathrm{d}G(r),$$

with G a uniquely determined nonnegative measure. Rephrased, g is the Laplace transform of G. This fact completes the proof by noting that positive definite functions are closed under scale mixtures.

B. Validity of the model given in Example 4.1

Let f be a Bernstein function. The following model is valid covariance function on $\mathbb{R}^d \times \mathbb{S}^1$ (see Alegría et al., 2017)

$$C_Y(\boldsymbol{h}, u_c) = \frac{1}{\{f(u_c)|_{[0,\pi]}\}^{d/2}} \exp\left(-\frac{\|\boldsymbol{h}\|^2}{f(u_c)|_{[0,\pi]}}\right).$$

Consider $\boldsymbol{V} \sim \mathcal{N}(\boldsymbol{\mu}, \Lambda/2)$. Thus, covariance (4.2) is given by

$$\begin{aligned} C(\boldsymbol{h}, u_l, u_c) &= \mathbb{E}_V\{C_Y(\boldsymbol{h} - u_l\boldsymbol{V}, u_c)\} \\ &= \frac{(2\pi)^{-d/2}|\Lambda/2|^{-1/2}}{\{f(u_c)|_{[0,\pi]}\}^{d/2}} \int_{\mathbb{R}^d} \exp\left(-\frac{\|\boldsymbol{h} - u_l\boldsymbol{v}\|^2}{f(u_c)|_{[0,\pi]}}\right) \exp\left(-(\boldsymbol{v}-\boldsymbol{\mu})^\top \Lambda^{-1}(\boldsymbol{v}-\boldsymbol{\mu})\right) \mathrm{d}\boldsymbol{v}. \end{aligned}$$

Using standard results on Gaussian mixtures (see Schlather, 2011) we have that

$$C(\boldsymbol{h}, u_l, u_c) = \frac{\left|\frac{u_l^2}{f(u_c)|_{[0,\pi]}}\Lambda + I_d\right|^{-1/2}}{(2\pi)^{d/2} f(u_c)|_{[0,\pi]}{}^{d/2}} \exp\left(-\frac{1}{f(u_c)|_{[0,\pi]}}(\boldsymbol{h} - u_l\boldsymbol{\mu})^\top \left(\frac{u_l^2}{f(u_c)|_{[0,\pi]}}\Lambda + I_d\right)^{-1} (\boldsymbol{h} - u_l\boldsymbol{\mu})\right).$$

The last expression coupled with Bernstein's Theorem (Feller, 1966) imply the result.

C. Proof of Theorem 6.1

We first introduce the spherical harmonics functions (see Marinucci and Peccati, 2011). Let $n \in \mathbb{N}$ and denote $\mathcal{Y}_{n,m,d}$, for $m = 1, \ldots, N_n(d)$, the spherical harmonics of degree n. Such mappings form an orthogonal basis of $L^2(\mathbb{S}^d; \omega_d)$, where ω_d is the surface area measure of $\mathbb{S}^d$.

The sufficient part of Theorem 6.1 can be obtained by defining the field

$$Z(\boldsymbol{x}, t_l, \boldsymbol{t}_c) = \sum_{n=0}^{\infty} \sum_{k=0}^{\infty} \sum_{m=1}^{N_n(d)} \sum_{\ell=1}^{N_k(1)} X_{n,k,m,\ell}(t_l) \mathcal{Y}_{n,m,d}(\boldsymbol{x}) \mathcal{Y}_{k,\ell,1}(\boldsymbol{t}_c),$$

for $(\boldsymbol{x}, t_l, \boldsymbol{t}_c) \in \mathbb{S}^d \times \mathbb{R} \times \mathbb{S}^1$, where $\{X_{n,k,m,\ell}\}$ is a collection of stochastic processes on the real line such that

$$\mathrm{cov}\{X_{n,k,m,\ell}(t_l + u_l), X_{n',k',m',\ell'}(t_l)\} = \delta_n^{n'} \delta_k^{k'} \delta_m^{m'} \delta_\ell^{\ell'} \varphi_{n,k}(u_l),$$

where $\delta_n^{n'} = 1$, if $n = n'$, and $\delta_n^{n'} = 0$, otherwise. Addition theorem for spherical harmonics (see Marinucci and Peccati, 2011) implies that the covariance of Z is given by (6.1).

The necessary part is obtained using similar arguments as in Ma (2016). In particular, we mix the arguments given in the proof of parts (i) and (ii) of Theorem 2 of Ma (2016). We define the following field on the real line

$$V_{n,k}(t_l) = \frac{1}{\pi}\int_{\mathbb{S}^d}\int_0^{2\pi} Z(\boldsymbol{x}, t_l, \boldsymbol{t}_c)\cos(n\xi)\mathcal{G}_k^{(d-1)/2}(\langle \boldsymbol{x}, \boldsymbol{\lambda}\rangle)\mathrm{d}\xi\mathrm{d}\boldsymbol{x},$$

where $\boldsymbol{t}_c = (\cos\xi, \sin\xi)^\top \in \mathbb{S}^1$ and $\boldsymbol{\lambda}$ is a random vector uniformly distributed on $\mathbb{S}^d$. A straightforward calculation shows that $\mathrm{cov}\{V_{n,k}(t_l + u_l), V_{n,k}(t_l)\}$ is positively proportional to $\varphi_{n,k}(u_l)$. So that, $\varphi_{n,k}$ is a stationary covariance function on the real line, for any n and k.

References

Abramowitz, M. and Stegun, I. A., editors (1970). *Handbook of Mathematical Functions*. Dover, New York.

Alegria, A. and Porcu, E. (2016). The dimple problem related to space-time modeling under the Lagrangian framework. *arXiv preprint arXiv:1611.09005*.

Alegría, A., Porcu, E., Furrer, R., and Mateu, J. (2017). Covariance Functions for Multivariate Gaussian Fields evolving temporally over Planet Earth. *ArXiv e-prints*.

Berg, C. and Porcu, E. (2016). From Schoenberg coefficients to Schoenberg functions. *Constructive Approximation*, To Appear.

Bochner, S. (1955). *Harmonic Analysis and the Theory of Probability*. California Monographs in mathematical sciences. University of California Press.

Cox, D. and Isham, V. (1988). A simple spatial-temporal model of rainfall. *Proceedings of the Royal Society of London Series A*, 415:317–328.

Cressie, N. and Wikle, C. K. (2015). *Statistics for spatio-temporal data*. John Wiley & Sons.

Daley, D. and Porcu, E. (2014). Dimension walks and Schoenberg spectral measures. *Proceedings of the American Mathematical Society*, 142(5):1813–1824.

Daley, D., Porcu, E., and Bevilacqua, M. (2015). Classes of compactly supported covariance functions for multivariate random fields. *Stochastic Environmental Research and Risk Assessment*, 29(4):1249–1263.

Feller, W. (1966). *An introduction to probability theory and its applications*. Number v. 2 in Wiley mathematical statistics series. Wiley.

Fuentes, M., Chen, L., and Davis, J. M. (2008). A class of nonseparable and nonstationary spatial temporal covariance functions. *Environmetrics*, 19(5):487–507.

Gent, P. R., Danabasoglu, G., Donner, L. J., Holland, M. M., Hunke, E. C., Jayne, S. R., Lawrence, D. M., Neale, R. B., Rasch, P. J., Vertenstein, M., Worley, P. H., Yang, Z.-L., and Zhang, M. (2011). The community climate system model version 4. *Journal of Climate*, 24(19):4973–4991.

Gneiting, T. (2002). Nonseparable, stationary covariance functions for space–time data. *Journal of the American Statistical Association*, 97(458):590–600.

Gneiting, T. (2013). Strictly and non-strictly positive definite functions on spheres. *Bernoulli*, 19(4):1327–1349.

Gneiting, T., Genton, M. G., and Guttorp, P. (2007). Geostatistical space-time models, stationarity, separability and full symmetry. In Finkenstadt, B., Held, L., and Isham,

V., editors, *Statistical Methods for Spatio-Temporal Systems*, pages 151–175. Chapman & Hall/CRC, Boca Raton: FL.

Guella, J., Menegatto, V., and Peron, A. P. (2015). An extension of a theorem of Schoenberg to products of spheres. *arXiv preprint arXiv:1503.08174*.

Gupta, V. K. and Waymire, E. (1987). On Taylor's hypothesis and dissipation in rainfall. *Journal of Geophysical Research: Atmospheres*, 92(D8):9657–9660.

Haslett, J. and Raftery, A. E. (1989). Space-time modelling with long-memory dependence: Assessing ireland's wind power resource (with discussion). *Applied Statistics*, 38:1–50.

Ma, C. (2016). Time varying isotropic vector random fields on spheres. *Journal of Theoretical Probability*, To Appear.

Marinucci, D. and Peccati, G. (2011). *Random fields on the sphere: representation, limit theorems and cosmological applications*, volume 389. Cambridge University Press.

Porcu, E., Bevilacqua, M., and Genton, M. G. (2016). Spatio-temporal covariance and cross-covariance functions of the great circle distance on a sphere. *Journal of the American Statistical Association*, 111(514):888–898.

Porcu, E. and Schilling, R. L. (2011). From Schoenberg to pick–nevanlinna: Towards a complete picture of the variogram class. *Bernoulli*, 17(1):441–455.

Schlather, M. (2011). Some covariance models based on normal scale mixtures. *Bernoulli*, 16:780–797.

Shirota, S. and Gelfand, A. E. (2016). Space and Circular Time Log Gaussian Cox Processes with Application to Crime Event Data. *Annals of Applied Statistics*, To Appear.

Stein, M. L. (2005). Space: Time covariance functions. *Journal of the American Statistical Association*, 100(469):310–321.

Zhang, H. and Wang, Y. (2010). Kriging and cross-validation for massive spatial data. *Environmetrics*, 21(3-4):290–304.